

You might find this additional information useful...

This article cites 43 articles, 24 of which you can access free at:

<http://jn.physiology.org/cgi/content/full/92/4/2137#BIBL>

This article has been cited by 7 other HighWire hosted articles, the first 5 are:

Plasticity between Neuronal Pairs in Layer 4 of Visual Cortex Varies with Synapse State

I. Saez and M. J. Friedlander

J. Neurosci., December 2, 2009; 29 (48): 15286-15298.

[\[Abstract\]](#) [\[Full Text\]](#) [\[PDF\]](#)

Synaptic Output of Individual Layer 4 Neurons in Guinea Pig Visual Cortex

I. Saez and M. J. Friedlander

J. Neurosci., April 15, 2009; 29 (15): 4930-4944.

[\[Abstract\]](#) [\[Full Text\]](#) [\[PDF\]](#)

Shift in the Balance between Excitation and Inhibition during Sensory Adaptation of S1 Neurons

J. E. Heiss, Y. Katz, E. Ganmor and I. Lampl

J. Neurosci., December 3, 2008; 28 (49): 13320-13330.

[\[Abstract\]](#) [\[Full Text\]](#) [\[PDF\]](#)

Subcolumnar Dendritic and Axonal Organization of Spiny Stellate and Star Pyramid Neurons within a Barrel in Rat Somatosensory Cortex

V. Egger, T. Nevian and R. M. Bruno

Cereb Cortex, April 1, 2008; 18 (4): 876-889.

[\[Abstract\]](#) [\[Full Text\]](#) [\[PDF\]](#)

Cross-Whisker Adaptation of Neurons in the Rat Barrel Cortex

Y. Katz, J. E. Heiss and I. Lampl

J. Neurosci., December 20, 2006; 26 (51): 13363-13372.

[\[Abstract\]](#) [\[Full Text\]](#) [\[PDF\]](#)

Updated information and services including high-resolution figures, can be found at:

<http://jn.physiology.org/cgi/content/full/92/4/2137>

Additional material and information about *Journal of Neurophysiology* can be found at:

<http://www.the-aps.org/publications/jn>

This information is current as of May 31, 2010 .

Functional Connectivity in Layer IV Local Excitatory Circuits of Rat Somatosensory Cortex

Anna I. Cowan^{1,2} and Christian Stricker^{1,2,3}

¹Institute of Neuroinformatics, University of Zürich and Federal Institute of Technology (Eidgenössische Technische Hochschule), CH-8057 Zürich, Switzerland; ²Division of Neuroscience, John Curtin School of Medical Research, Canberra, ACT 0200; and ³Australian National University Medical School, Canberra, ACT 0200, Australia

Submitted 24 December 2003; accepted in final form 10 June 2004

Cowan, Anna I. and Christian Stricker. Functional connectivity in layer IV local excitatory circuits of rat somatosensory cortex. *J Neurophysiol* 92: 2137–2150, 2004. First published June 16, 2004; 10.1152/jn.01262.2003. There are two types of excitatory neurons within layer IV of rat somatosensory cortex: star pyramidal (SP) and spiny stellate cells (SS). We examined the intrinsic properties and connectivity between these neurons to determine differences in function. Eighty-four whole cell recordings of pairs of neurons were examined in slices of rat barrel cortex at $36 \pm 1^\circ\text{C}$. Only minimal differences in intrinsic properties were found; however, differences in synaptic strength could clearly be shown. Connections between homonymous pairs (SS–SS or SP–SP) had a higher efficacy than heteronymous connections. This difference was mainly a result of quantal content. In 42 pairs, synaptic dynamics were examined. Sequences of action potentials (3–20 Hz) in the presynaptic neuron consistently caused synaptic depression ($E_2/E_1 = 0.53 \pm 0.18$). The dominant component of depression was release-independent; this depression occurred even when preceding action potentials had failed to cause a response. The release-dependence of depression was target specific; in addition, release-independence was greater for postsynaptic SPs. In a subset of connections formed only between SP and any other cell type (43%), synaptic efficacy was dependent on the presynaptic membrane potential (V_m); at -55 mV, the connections were almost silent, whereas at -85 mV, transmission was very reliable. We suggest that, within layer IV, there is stronger efficacy between homonymous than between heteronymous excitatory connections. Under dynamic conditions, the functional connectivity is shaped by synaptic efficacy at individual connections, by V_m , and by the specificity in the types of synaptic depression.

INTRODUCTION

It is universally accepted that there is an active role for intracortical circuitry in processing sensory signals. However, detailed analysis of the synaptic mechanisms underlying intracortical connections lags behind the understanding of both the anatomy and the physiology of synaptic transmission in other brain areas (e.g., hippocampus and cerebellum).

The barrel cortex (S1) is the first stage in cortical processing for thalamocortical signals, which are initiated by movements of the whiskers on a rat's muzzle. The thalamocortical fibers make synapses mainly in layer IV, the input layer for somatosensory signals (Keller 1995; White 1978). Within this layer, there are two dominant types of excitatory neurons: star pyramidal (SP) and spiny stellate (SS) cells. This is an unusual situation, in that in other cortical layers,

excitatory neurons are mainly of the classical pyramidal type (Keller 1995).

SS and SP cells have quite different morphological characteristics, the most obvious of these is that the latter have a prominent apical dendrite, which may or may not extend into layer II/III (Elston et al. 1997; Keller 1995; Lübke et al. 2000; Peters and Kara 1985; Simons and Woolsey 1984; White 1978). SS cells do not, in general, have an apical-basal orientation of the dendritic arbour, and all dendrites are of approximately equal length. It has been suggested that SS cells are modified SP cells, where the apical dendrite has atrophied during development (Amitai and Connors 1995; Peinado and Katz 1990; Vercelli et al. 1992). However, the existence of two types of excitatory neuron within layer IV, even in adult animals, prompts the question of whether the physiological and functional properties of these two classes of neurons are the same or whether they have the potential to play different roles in cortical processing of sensory information.

To address this question, we examined the basic electrophysiological characteristics of SS and SP cells, as well as aspects of synaptic transmission within the local circuits in layer IV. Based on intrinsic properties of SS and SP cells alone, the two cell groups could not be distinguished from each other. However, there was specificity in the synaptic strength at the various types of connections. The synaptic strength at homonymous connections was greater than that of heteronymous connections. In addition, short-term synaptic depression showed target specificity.

METHODS

Slice preparation

Fourteen- to 18-day-old Wistar rats of either sex were killed by decapitation, and parasagittal (Simkus and Stricker 2002) or thalamocortical (Agmon and Connors 1991; Feldmeyer et al. 1999) slices were prepared. The techniques used were approved by the Department for Veterinary Affairs of the Canton of Zürich, Switzerland. The artificial cerebrospinal fluid (ACSF) contained (in mM) 125 NaCl, 2.5 KCl, 25 NaHCO₃, 1.25 NaH₂PO₄, 2.0 CaCl₂, 1.0 MgCl₂, and 25.0 glucose, gassed with 95% O₂-5% CO₂ (pH 7.4). In most cases, 10 μM bicuculline methiodide was added to block GABA_A-mediated inhibitory transmission. All experiments were conducted at $36 \pm 1^\circ\text{C}$. The intracellular solution contained (in mM) 115 K-gluconate, 20 KCl, 10

Address for reprint requests and other correspondence: C. Stricker, Div. of Neuroscience, JCSMR-ANU, GPO Box 334, Canberra, ACT 0200, Australia (E-mail: Christian.Stricker@anu.edu.au).

The costs of publication of this article were defrayed in part by the payment of page charges. The article must therefore be hereby marked "advertisement" in accordance with 18 U.S.C. Section 1734 solely to indicate this fact.

HEPES, 10 phosphocreatine, 4 Mg-ATP, 0.3 Na-GTP, and 0.25% biocytin (pH 7.2; osmolarity, 305 mOsm).

Recording

Patch pipettes were pulled from thick-walled borosilicate glass (Hilgenberg, Malsfeld, Germany) and had a tip resistance of 3–5 M Ω . Neurons in layer IV of somatosensory cortex were visualized with infrared DIC video microscopy (Dodt and Zieglgänsberger 1990). Paired recordings between connected neurons in layer IV were obtained by sequentially obtaining whole cell recordings between pairs of neurons and testing for a synaptic connection in both directions. A “loose-patch” technique (Feldmeyer et al. 1999) was not used to search for potential pairs, because it was determined in preliminary experiments that this could bias the connections toward those of larger amplitudes and high probability. Once a connection had been found, the presynaptic neuron was recorded in current clamp (Axoclamp 2B, Axon Instruments), and the postsynaptic neuron was held in voltage-clamp at -70 mV (Axopatch 200B). Access resistance was 12.3 ± 3.6 M Ω and was uncompensated. Short current pulses (0.2–0.5 nA for 5 ms) were used to evoke action potentials in the presynaptic neuron (rate, 0.1–0.5 Hz for investigation of basic synaptic parameters and quantal analysis; bursts of 3–20 Hz for synaptic dynamics evoked by trains of ≤ 20 action potentials with an interburst interval of 15 s). Both the presynaptic action potentials and the excitatory postsynaptic currents (EPSCs) evoked in the postsynaptic neuron were recorded. In subsequent notation, the direction within a paired recording is given by specifying the presynaptic neuron first.

The membrane currents were amplified (100–500 times) following a sample-and-hold step to ensure that the full resolution of the AD converter could be utilized (custom-built sample-and-hold amplifier, design JCSMR, ANU, Australia). The signal was filtered at 2 kHz and digitized at 5 kHz using an ITC-18 computer interface (Instrutech, Port Washington, NY). Data were acquired using software developed with IGOR Pro 4.0 (Wavemetrics).

Histology

The identification of all neurons was performed histologically. The procedures followed those of Horikawa and Armstrong (1988). Briefly, the slices were fixed in 4% paraformaldehyde for ≥ 2 h and washed in 0.1 M phosphate buffer. They were incubated with avidin- and biotin-conjugated horseradish peroxidase (ABC Elite Kit, Vectastain) for 24–48 h in Tris buffer containing 0.5% triton, reacted with phenylenediamine (Sigma), and intensified with nickel and cobalt. Hydrogen peroxide (0.003%) was added, and the slices were left until the desired staining was achieved. Finally, the slices were mounted on slides and dehydrated through an alcohol series. The criteria for determining whether a neuron was an SS cell, SP cell, or an inhibitory interneuron were as described elsewhere (Elston et al. 1997; Keller 1995; Lübke et al. 2000; Peters and Kara 1985; Simons and Woolsey 1984; White 1978). Note that all neurons in this study with an apical dendrite extending out of layer IV are classified as SP cells, without the subclassification of pyramid/SP cells (Schubert et al. 2003).

Analysis

The peak amplitude and latency of individual EPSCs were measured manually together with an estimate of the noise according to the method described in Stricker et al. (1996). For all connections, the average peak amplitude, coefficient of variation (CV), skew, and noise variance (σ_n) were determined. The skew was calculated as follows

$$\text{skew} = \frac{1}{N} \sum_{i=1}^N \left(\frac{E_i - \bar{E}}{\sigma} \right)^3$$

where i is the trial number, N is the total number of trials, E represents the amplitude of an individual EPSC, \bar{E} is the average, and σ is the SD of the sample.

Probability density functions (PDFs) of the EPSC amplitudes were constructed by convolving each peak amplitude value with a Gaussian of the size described in Stricker et al. (1994). The advantage of using a Gaussian kernel lies in the fact that, given a limited sample size of 300–500 EPSCs, the underlying density is more efficiently represented than when binned data sets are used (for details, see Silverman 1986). In addition, there is a bias introduced into the formation of the density by deciding on the bin width and the centering of the bin. The proportion of failures (i.e., the probability of the component centered around 0) was determined from the PDFs directly.

Synaptic depression was quantified as the ratio between the mean of the second EPSCs (\bar{E}_2) and that of the first EPSCs (\bar{E}_1) for each experiment. The release-dependence of synaptic depression was analyzed according to the methods described in Fuhrmann et al. (2004). Briefly, a release-dependence factor (R_D) was calculated for each connection according to

$$R_D = \frac{a - \bar{E}_2}{\bar{E}_1 - \bar{E}_2} \quad (1)$$

where a is the y -intercept of the linear regression for a plot of E_2 versus E_1 , and the bar indicates the average over the whole sample. Analysis of covariance (ANCOVA) was used to determine the significance of the difference between the y -intercept and slope of the regression line, with predicted lines describing pure release-dependent ($R_D = 1$) and -independent ($R_D = 0$) mechanisms. In all cases, R_D was calculated for a stimulus frequency of 20 Hz.

Quantal analysis was performed on a subset of connections according to the methods described in Stricker et al. (1994). Briefly, the data were checked for stationarity. Then, the PDFs were first tested against the null hypothesis that the PDF was the result of a unimodal process (gamma, Weibull, double Gaussian, and cubic transform of a Gaussian variable). If this null hypothesis (H_0) could be rejected, models of transmission with an increasing number of constraints (complexity) were systematically tested against less complex models. The models considered were 1) a quantal model where the normal distributions in the mixture model are separated by a constant increment (the quantal amplitude, Q); 2) a quantal model as in 1) but with quantal variance added to the noise variance; 3) a quantal model with binomial (uniform) release probabilities, with or without quantal variance; and 4) a quantal model with compound (nonuniform) binomial release probabilities, with or without quantal variance.

Each of these models of transmission had their parameters adjusted to maximize the likelihood of the fit to the PDF. Complete details on how competing models of transmission were evaluated are given in Stricker et al. (1994). Once the most appropriate model of transmission was determined, the quantal current (Q), quantal content ($m = \bar{E}/Q$), the coefficient of variation of the quantal response (CV_Q), where necessary, and the probability of failures (P_0) were extracted. Confidence limits of each parameter were determined using a balanced bootstrap scheme. Since we were unable to assign a probability of transmitter release to most of the connections, we resorted to using failure rate, paired-pulse ratio as well as estimating the skew of the density to indicate whether the synapse had a high or low release probability (see Fig. 4). In short, for a binomial process with $P = 0.5$, the skew is zero; however, if $P > 0.5$, the skew is negative, and for $P < 0.5$, it is positive. This consideration applies for EPSCs, which are measured as inward currents (negative values).

Statistical significance in the characteristics of synaptic transmission and dynamics in different populations of neurons were examined using a Student's t -test ($P_t \leq 0.05$). Group data are expressed as

mean \pm SD. Statistical significance of comparison between models of transmission is given by P_{MC} , when based on Monte Carlo simulations, or P_{χ^2} , when based on χ^2 statistics (Stricker et al. 1994).

RESULTS

Positive identification of all neurons was based on their anatomical characteristics (Elston et al. 1997; Keller 1995; Lübke et al. 2000; Peters and Kara 1985; Simons and Woolsey 1984; White 1978). SS cells typically had a round cell body and a dendritic arbour, which did not have a clear apical-basal orientation (see Fig. 1A). In contrast, the somata of SP cells were pyramidally shaped; they had a prominent apical dendrite and a basal dendritic spray. According to this definition, the dendrites of either cell type can have an asymmetric orientation in relation to the barrel walls. Spiny neurons were considered inhibitory without further classification.

Electrical properties

To determine basic cellular properties and whether there were any distinguishing electrophysiological properties between excitatory cell types, we recorded from 40 individual cells in layer IV. Inhibitory neurons could easily be distinguished from excitatory neurons based on their high input resistance ($R_{in} = 421 \pm 43 \text{ M}\Omega$, $n = 7$), a fast action potential (height: $90.9 \pm 9.7 \text{ mV}$; half-width: $1.2 \pm 0.1 \text{ ms}$) followed by a pronounced afterhyperpolarization (AHP), and a high regular firing frequency ($>100 \text{ Hz}$). Except for action potential amplitude, all these characteristics were significantly different from those of excitatory neurons ($P_t < 0.02$).

The two excitatory neuronal types were indistinguishable by most electrophysiological characteristics. For SS and SP cells, V_m (-68.3 ± 4.2 and $-67.1 \pm 5.1 \text{ mV}$, respectively), action potential height (88.4 ± 2.2 and $96.0 \pm 4.2 \text{ mV}$, respectively),

half-width (1.9 ± 0.1 and $1.8 \pm 0.1 \text{ ms}$, respectively), and R_{in} (242 ± 38 and $241 \pm 53 \text{ M}\Omega$, respectively) were not significantly different. Both cell types displayed regular firing patterns and fired at similar frequencies for small currents injected. However, when larger currents were injected, the action potentials of SS cells tended to inactivate earlier than those of SP cells (Fig. 1, B and C). The firing rate was significantly different for currents $\geq 0.4 \text{ nA}$ ($P_t < 0.05$). However, this property could not be used to unambiguously identify the two types because of the large variance within each group. Since we observed no difference in either R_{in} or V_m for the two cell types, the inactivation was not a result of systematic changes in these parameters.

Synaptic properties

To examine whether we had sufficient resolution to detect even small postsynaptic responses, we recorded from a number of connections of small average amplitude in both voltage- and current-clamp mode. We defined the resolution threshold for EPSCs to be 2.5 times the SD of the noise (σ_n , see also Jack et al. 1981). An example is shown in Fig. 2, where 44% of responses recorded from the same cell pair were detectable above noise (0.7 pA) in voltage-clamp mode, but only 13% (52 μV) in current-clamp mode. Given such an improved resolution, we decided to routinely record in voltage-clamp mode.

The major part of this report is based on whole cell recordings from 84 pairs of connected layer IV neurons. All connected pairs were located within the same barrel, and all were within $<100 \mu\text{m}$ of each other (usually $<50 \mu\text{m}$). Within this limited data set, there were no location specific differences in basic synaptic transmission or short-term dynamics. An overview of these 84 pairs is given in Table 1. The rate of connectivity between cell pairs tested was about 25%, and

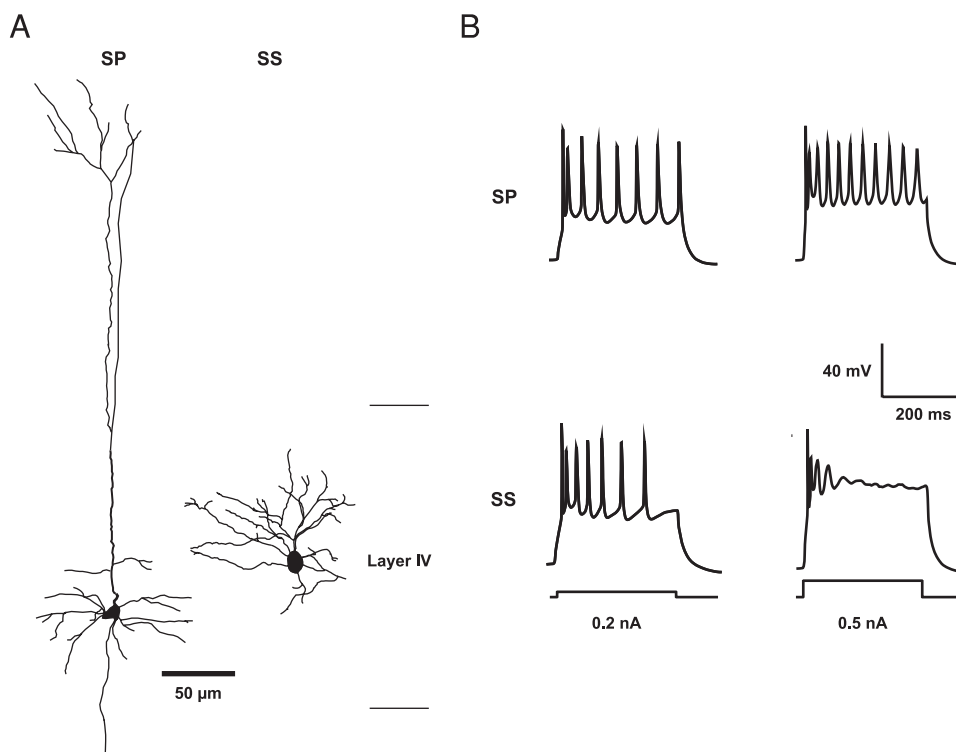


FIG. 1. Morphology and firing patterns of layer IV excitatory neurons. A: 2 reconstructed cells, star pyramidal (SP) on the left with long apical dendrite and spiny stellate cells (SS) to the right with radiating dendrites in layer IV. B: typical examples of the firing pattern of an SP (top) and an SS (bottom) in response to 2 different current amplitudes.

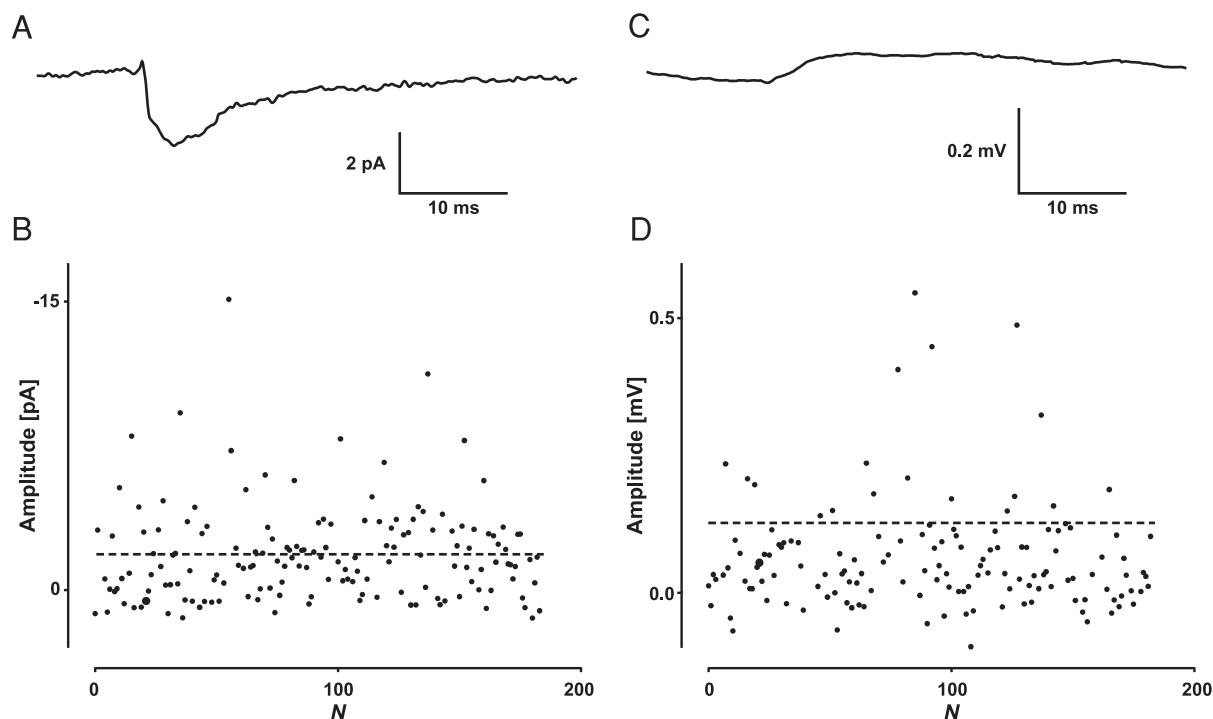


FIG. 2. Recording mode. Example of the same small amplitude connection recorded in voltage and current clamp. *A* and *B*: voltage-clamp recording. Average excitatory postsynaptic current (EPSC; *A*) is clearly visible above the noise, and in 44% of the individual trials, an EPSC can be distinguished (*B*). *C* and *D*: current-clamp recording of the same postsynaptic response. Average excitatory postsynaptic potential (EPSP; *C*) is visible above the noise after many trials, but only in 13% of the individual sweeps can an EPSP be resolved (*D*). Dashed line in *C* and *D* indicates $2.5 \times \sigma_n$ (detection threshold; 70 pA in *C* and 52 μV in *D*).

reciprocal connections were found in about 20% of these connected cell pairs. The average EPSC amplitude was -11.7 ± 11.3 pA, and the CV was 0.8 ± 0.5 . The average failure rate (P_0) was $12 \pm 13\%$, and the skew was 0.4 ± 1.0 . The characteristics of synaptic transmission at these connections covered a wide range: from small-amplitude, low-probability connections with a high percentage of transmission failures (smallest amplitude: -0.7 ± 1.6 pA; $P_0 = 60\%$; skew = 2.5) to connections where the synaptic strength was much higher (largest amplitude = -47.9 ± 7.3 pA; no failures; skew = -0.7).

HOMONYMOUS AND HETERONYMOUS CONNECTIONS. We analyzed the data to determine whether there were any differences in the efficacy of these two types of connections. It was a highly consistent finding that homonymous connections (i.e.,

connections between 2 neurons of the same type) were stronger than heteronymous connections (connections between different neuronal types) as indicated by the fact that the proportion of transmission failures was smaller (7 ± 8 vs. $18 \pm 15\%$, $P_t < 0.0002$; Table 1), and the average skew was more negative for homonymous connections (0.0 ± 0.6 vs. 0.8 ± 1.2 , $P_t < 0.001$; Table 1), consistent with a higher release probability (see *Short-term synaptic depression*).

Short-term synaptic depression

Short-term synaptic dynamics were investigated at 42 excitatory-excitatory connections. Within the range of frequencies from 3 to 20 Hz, all connections consistently showed synaptic depression (average $\bar{E}_2/\bar{E}_1 = 0.53 \pm 0.18$; Table 2). The

TABLE 1. Properties of types of connections

Cell Type	<i>N</i>	\bar{E} , pA	<i>RT</i> , ms	<i>HW</i> , ms	<i>CV</i>	P_0 , %	Skew
SS-SS	11	-13.1 ± 11.0	2.0 ± 1.1	9.8 ± 13.2	0.5 ± 0.2	7 ± 8	0.1 ± 0.6
SS-SP	17	-9.2 ± 11.8	1.8 ± 0.7	5.6 ± 2.4	0.9 ± 1.7	20 ± 14	0.9 ± 1.7
SP-SP	33	-13.5 ± 10.5	1.8 ± 0.6	7.5 ± 3.7	0.5 ± 0.3	7 ± 8	0.0 ± 0.6
SP-SS	23	-8.4 ± 10.6	1.7 ± 0.5	6.6 ± 2.4	0.9 ± 0.5	18 ± 16	0.7 ± 0.8
Homonymous	44	-13.4 ± 10.5	1.9 ± 0.8	7.4 ± 3.5	0.5 ± 0.2	7 ± 8	0.0 ± 0.6
Heteronymous	40	-9.6 ± 12.2	1.7 ± 0.6	6.2 ± 2.4	$1.0 \pm 0.6^*$	$18 \pm 15^*$	$0.8 \pm 1.2^*$
Presynaptic SS	28	-10.8 ± 11.4	1.9 ± 0.9	7.4 ± 8.8	0.9 ± 0.7	15 ± 14	0.6 ± 1.4
Presynaptic SP	56	-11.4 ± 11.5	1.8 ± 0.5	7.1 ± 3.2	0.7 ± 0.4	12 ± 13	0.2 ± 0.8
Postsynaptic SS	34	-10.0 ± 10.8	1.8 ± 0.8	7.9 ± 8.6	0.8 ± 0.5	15 ± 15	0.5 ± 0.8
Postsynaptic SP	50	-12.1 ± 11.0	1.8 ± 0.6	6.8 ± 3.4	0.7 ± 0.6	11 ± 12	0.3 ± 1.2
All	84	-11.7 ± 11.3	1.8 ± 0.7	7.2 ± 5.9	0.8 ± 0.5	12 ± 13	0.4 ± 1.0

Values are means \pm SE. *Signifies statistically different from the previous value at $P_t < 0.0005$. SS, spiny stellate cell; SP, star pyramid; *N*, number of connections; *RT*, 10–90% rise time of EPSCs; *HW*, half-width; *CV*, coefficient of variation; P_0 is the failure rate. Skew, skewness of the distribution.

TABLE 2. Summary of short-term synaptic depression

Cell Type	<i>N</i>	E_2/E_1	R_D
SS-SS	6	0.57 ± 0.23	0.36 ± 0.26
SS-SP	8	0.51 ± 0.21	0.13 ± 0.16
SP-SP	21	0.53 ± 0.14	0.30 ± 0.30
SP-SS	7	0.47 ± 0.20	$0.55 \pm 0.22^*$
Homonymous	27	0.54 ± 0.17	0.32 ± 0.28
Heteronymous	15	0.49 ± 0.20	0.33 ± 0.29
Presynaptic SS	14	0.54 ± 0.23	0.23 ± 0.23
Presynaptic SP	28	0.51 ± 0.15	0.37 ± 0.30
Postsynaptic SS	13	0.51 ± 0.23	0.49 ± 0.25
Postsynaptic SP	29	0.53 ± 0.16	$0.25 \pm 0.27^*$
All	42	0.53 ± 0.18	0.30 ± 0.29

Values are means \pm SD. *Statistically different from the previous value at $P < 0.05$. SS, spiny stellate cell; SP, star pyramid; *N*, number of connections; E_2/E_1 normalized amount of depression; R_D , release-dependence factor as defined in Fuhrmann et al. (2004). R_D of 1 implies complete release dependence. A connection with $R_D = 0$ is release-independent.

amount of paired pulse depression was not significantly different from the average for any of the types of excitatory-excitatory connections. In all cases, the amount of depression and its release-dependence (see below) did not vary dependent on input frequency (within this relatively small frequency range).

According to recent evidence, a significant component of synaptic depression in the cortex is release-independent (Fuhrmann et al. 2004). In Fig. 3, we show three individual sweeps (gray-coded), which in Fig. 3A, show that E_2 is small when E_1

is big and vice versa, whereas is Fig. 3B, the amplitude of E_2 is largely independent from E_1 . We estimated the release-dependence factor (R_D), which indicates the amount of release-dependence ($R_D = 1$) or -independence ($R_D = 0$) of depression. If a connection is fully release-dependent, the depression can solely be explained by vesicle depletion alone. Under these circumstances, a negative correlation between the first and the second EPSC is expected (Matveev and Wang 2000; Scheuss et al. 2002). We found that layer IV excitatory connections showed depression ranging from largely release-dependent (Fig. 3, A and B) to completely release-independent (Fig. 3, C and D). The mean R_D for a stimulus frequency of 20 Hz was 0.30 ± 0.29 , indicating that these connections are dominated by release-independent depression and not by depletion of vesicles (see Fuhrmann et al. 2004).

Since the existence of release-independent depression could potentially be a phenomenon related to whole cell recording (wash-out), we performed control experiments, in which action potentials were induced in the presynaptic neuron in cell-attached mode. In four experiments, neither the amount of depression ($\bar{E}_2/\bar{E}_1 = 0.65 \pm 0.10$), the skew of the amplitude distribution (0.12 ± 0.16), nor R_D (0.27 ± 0.30) was significantly different from when the presynaptic neuron was recorded in whole cell mode ($P_t > 0.2$ for all 3 parameters). Thus, we conclude that, similar to layer V pyramidal cells (Fuhrmann et al. 2004), wash-out of the intracellular contents of the presynaptic neuron was an unlikely factor in the expres-

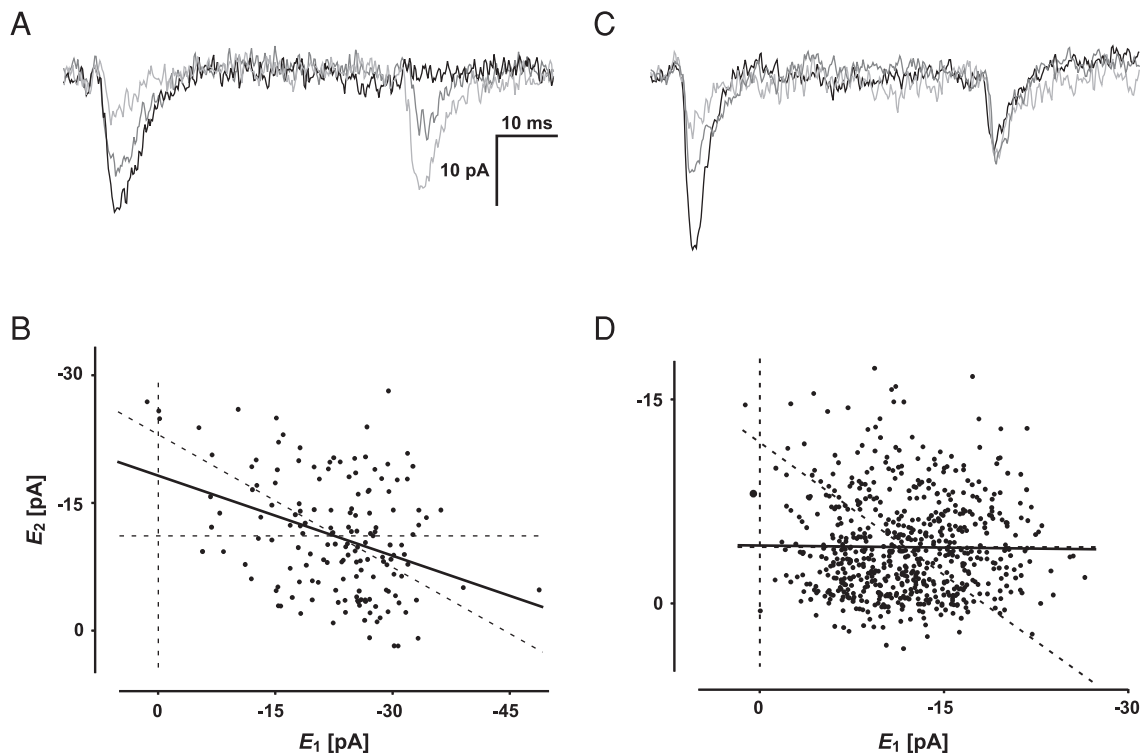


FIG. 3. Types of short-term synaptic depression. A: 3 individual EPSC traces (gray coded) from a SS-SS connection showing a high degree of release-dependence of short-term depression (stimulus frequency = 20 Hz). B: plot of E_2 vs. E_1 for the same connection as in A. There is a strong inverse correlation between the amplitude of E_2 and the amplitude of E_1 . Note, however, that theoretically complete release-dependence would require that the linear regression follow the dashed diagonal line. $R_D = 0.60 \pm 0.15$. C: individual EPSC traces from an SS-SP connection showing release-independent depression. D: plot of E_2 vs. E_1 for the same connection as in C. There is no correlation between the amplitude of E_1 and E_2 . $R_D = 0.02 \pm 0.05$. Dashed diagonal line, theoretical regression line for release-dependent depression; dashed horizontal line, theoretical regression line for release-independent depression.

sion of release-independent depression in layer IV SP and SS cells.

Within each type of connection examined, there was a wide range of values for R_D , such that in most cases, there was no significant difference among the groups. However, there was a significant difference in R_D between homo- and heteronymous connections when the presynaptic neuron was an SP cell ($P_t < 0.05$; Table 2). We found evidence for target cell specificity; there was a larger release-independent component to the depression when the postsynaptic neuron was an SP cell than when it was an SS cell (0.25 ± 0.27 vs. 0.49 ± 0.25 , $P_t < 0.05$; Table 2). This interpretation is corroborated by the significant difference in R_D between SP-SP and SP-SS connections (0.30 ± 0.30 vs. 0.55 ± 0.22 , $P_t < 0.05$) and a strong tendency for a similar finding in SS-SP and SS-SS connections (0.13 ± 0.16 vs. 0.36 ± 0.26 , $P_t = 0.06$; Table 2).

Release probability and type of depression

To elucidate whether the setting of a synapse had any influence on the form of depression observed, we needed to devise indirect measures since quantal analysis could not provide us with values for release probability (see *Quantal properties*) due to the fact that most distributions are overdispersed. We therefore calibrated the measure of skew with two other indices of release probability; i.e., failure rate and amount of paired-pulse depression. In a first set of analysis, we plotted paired-pulse ratio versus failure rate (P_0) and found that, in this data set, there was a significant correlation indicating that, for connections with zero failures, the largest amount of depression is observed ($r = 0.41$, $P_r = 0.01$; Fig. 4A). In a next step, we analyzed skew versus P_0 and again found that there was a significant correlation ($r = 0.49$; $P_r < 0.001$; Fig. 4B), indicating that a negative skew

is largely consistent with no failures. In a second set of analyses, the total amount of paired-pulse depression was also correlated with release probability ($r = 0.32$, $P_r = 0.05$; Fig. 4C), such that there was more depression for connections with a negative skew. We therefore suggest that a negative skew is consistent with a high, and a positive skew with a low release probability.

When we plotted R_D versus skew, we found that there was a correlation between R_D and the skew of the EPSC amplitude distribution ($r = -0.58$, $P_r < 0.01$; Fig. 4D), suggesting a relationship between release probability and the type of short-term synaptic depression. Those connections with high release probability (negative skew) were more likely to show release-dependent depression, whereas those neurons with lower release probability showed little or no release-dependent depression. The same holds true if R_D was plotted against paired-pulse ratio (data not shown). Thus it appears that only connections with high release probability express a significant degree of release-dependent depression.

Dependence of synaptic efficacy on presynaptic V_m

In a subset of connections, we found a novel mechanism by which synaptic efficacy could be modified significantly. This phenomenon was specific to a subset of connections where the presynaptic neuron was an SP cell and only occurred in about 43% of such cases (9 of 21 SP cells tested); SS cells do not show this phenomenon ($n = 16$). If V_m of the presynaptic neuron was altered by current injection in the range between -55 and -85 mV, the synaptic strength changed such that a connection with high probability of release, few release failures and large average amplitude at -85 mV became much weaker when the presynaptic neuron was more depolarized. An example is shown in Fig. 5, where the EPSC amplitudes (Fig.

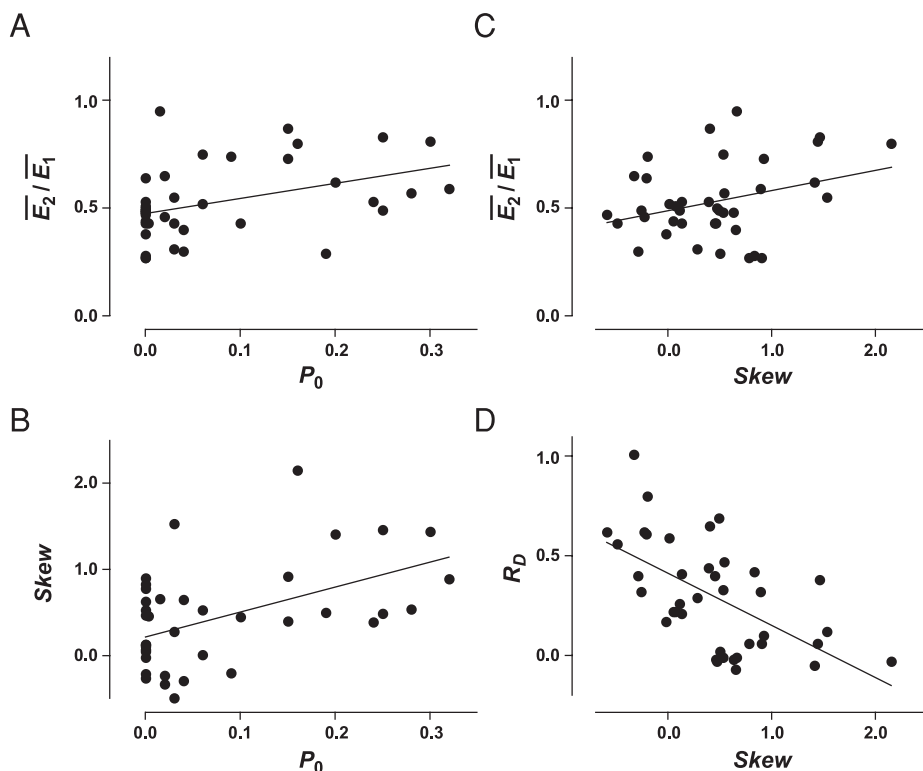


FIG. 4. Calibration of skew with failure rate and paired-pulse depression. *A*: correlation between paired-pulse depression (\bar{E}_2/\bar{E}_1) and failure rate ($r = 0.41$, $P_r < 0.01$). *B*: correlation between skew and failure rate ($r = 0.49$, $P_r < 0.01$). *C*: correlation between \bar{E}_2/\bar{E}_1 and skew. A greater degree of depression is correlated with a more negative skew (higher release probability; $r = 0.32$, $P_r = 0.05$). *D*: release-dependence of depression (R_D) is negatively correlated with the skew of the amplitude distribution, such that those connections with a negative skew (most likely high P synapses) have a tendency to show more release-dependent depression ($r = -0.58$, $P_r = 0.01$).

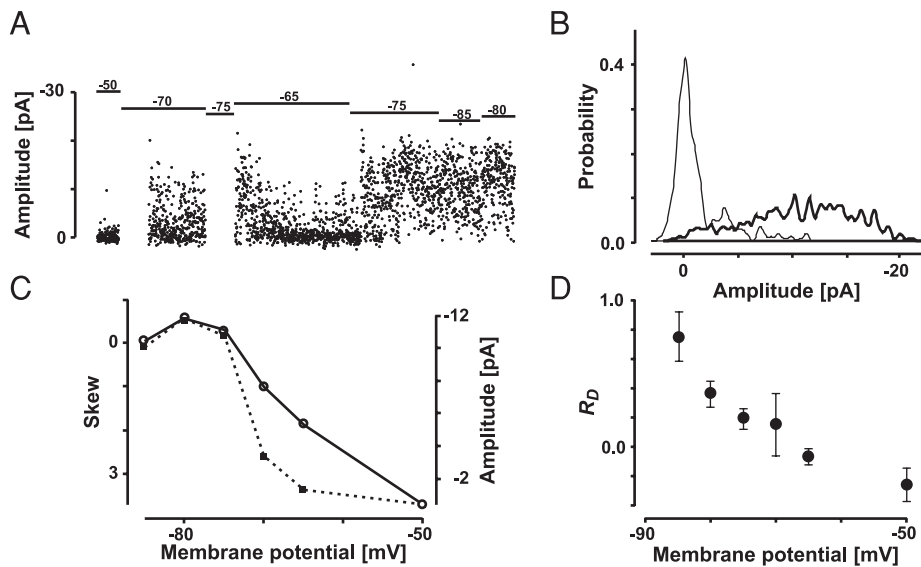


FIG. 5. Presynaptic membrane polarization and synaptic efficacy. In a subset of connections in which the presynaptic neuron is a SP, the synaptic efficacy varies as a result of changes in presynaptic V_m . A: varying V_m over the range -50 to -85 mV causes changes in the amplitude of EPSCs, such that the average EPSC amplitude is smaller at more depolarized potentials. This is shown in a plot of EPSC amplitude over time. Bars and numbers above trace indicate the presynaptic V_m induced by varying the DC current to the patch electrode. Note that for the 1st period at -70 and also at -75 mV, no recordings were taken. B: amplitude probability density functions (PDFs) for EPSCs recorded when V_m was -85 mV (dark line) and -65 mV (thin line). C: skew (\circ) and average amplitude (\blacksquare) plotted as a function of presynaptic V_m . D: R_D for the same connection plotted as a function of presynaptic V_m . Note that for V_m of -50 mV, this connection showed paired pulse facilitation, which explains why this point falls outside $0 \leq R_D \leq 1$.

5A), the resulting PDFs (Fig. 5B), the skew of the amplitude distribution, and average EPSC amplitude (Fig. 5C) all vary with the presynaptic V_m . There was no correlation between changes in action potential height or half-width and the change in efficacy. Also, note that the amplitudes of the EPSCs do not immediately follow the change in polarization; it takes time to reach a new steady state, and it takes longer when synaptic strength decreases (depolarization) than when it increases (hyperpolarization). The apparent time constants for the voltage steps are 6.8 ± 3.2 and 2.6 ± 2.2 min, respectively.

In addition, we investigated the release-dependence of synaptic depression in such neurons at different presynaptic V_m . We found that R_D changed from highly release-dependent at -85 mV to completely release-independent at -65 mV (Fig. 5D; $R_D = 0.80 \pm 0.18$ and 0.02 ± 0.03 , respectively). Whereas there was hardly any change in skew between -80 and -85 mV

(data not shown), there was a significant change in R_D (Fig. 6D), indicating that R_D is not a simple function reflecting release probability.

Quantal properties

To further investigate if synaptic efficacy was different between the two cell types and their connections, quantal analysis was performed on a subset of cell pairs where sufficiently long and stable recordings were taken to make this analysis feasible ($n = 28$). An example of a connection with relatively high release probability (negative skew) and few failures is shown in Fig. 6. The EPSC amplitudes (Fig. 6A), minute averages, R_{in} , and access resistance (R_A , Fig. 6B) were first determined to be stationary before proceeding to calculate the PDF (Fig. 3C, thin line), using a kernel size of 0.26 pA.

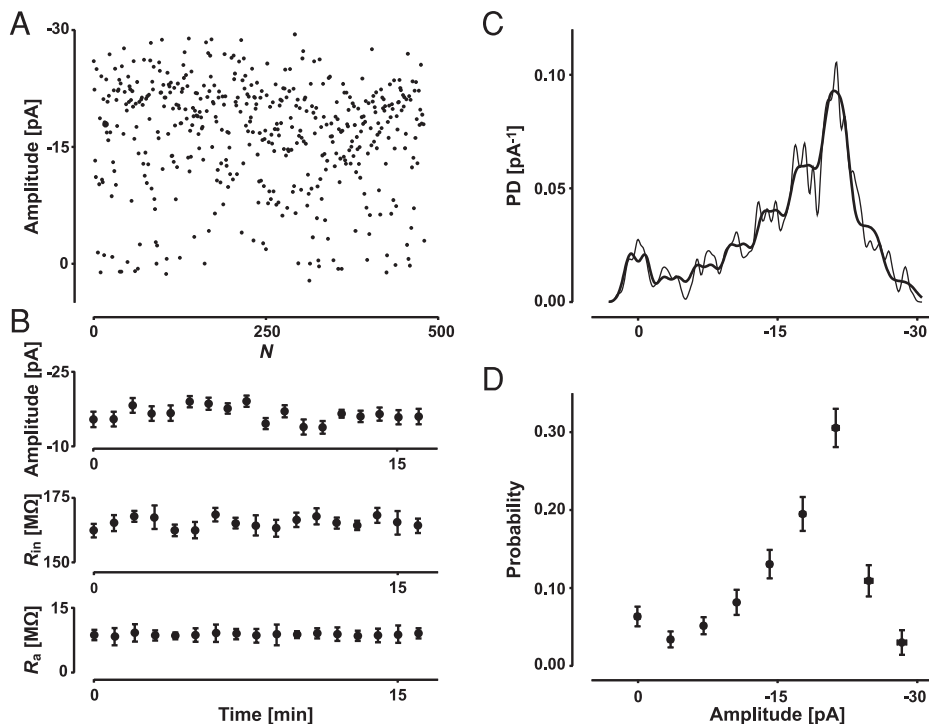


FIG. 6. Example of quantal analysis of a connection with high release probability. A: maximal amplitude of 463 individual EPSCs recorded at 0.5 Hz in an SS-SP (Table 3, *). B: minute averages of EPSC amplitude, R_{in} and R_A , displayed against time show stationarity of recording conditions. C: PDF (thin line) formed from the peak amplitudes of the EPSCs. Thick line is the optimal fit to the PDF. It is a quantal model with no constraints placed on the release process and with a CV_Q of 0.07 ± 0.02 . D: discrete amplitudes of the EPSCs, their locations, and associated probabilities together with confidence limits.

Four hundred sixty-three EPSCs contributed to this density, which had a mean of -16.6 ± 7.2 pA and $\sigma_n = 0.98$ pA. In a first step, a test was performed to assess if the density was indeed multimodal. To do that, the number of unevenly spaced noise components (K) contained in the PDF was identified as nine. This number indicates that if a 10th component were used to fit the PDF, there would be no significant increase in the goodness-of-fit. A number of unimodal hypotheses (gamma, Weibull, double Gaussian, and cubic transform; see METHODS) were tested against the multimodal case with $K = 9$. All unimodal hypotheses could be rejected at $P_{MC} \ll 0.004$.

Having established multimodality, we further tested if the modes were separated equally, which they would be if the process were quantized. Under the null-hypothesis that the modes were quantized, we obtained a quantal size $Q = -3.5$ pA ($P_\chi = 0.27$). We then examined whether quantal variability (intrasite variability) improved the fitting and found that it did require a CV_Q of 0.07 ($P_\chi = 0.04$). Next, we tested if a classical release process could account for the PDF. Qualitatively, this is very unlikely, since there are too many failures compared with the overall shape of the PDF; in fact, the failures make up an additional mode, which is incompatible with a binomial process. The statistical analysis confirms this by rejecting a binomial process at $P_{MC} < 0.004$. Therefore the model that best fits the PDF (Fig. 6, C, thick line, and D: see METHODS) was a quantal model ($Q = -3.6 \pm 0.1$) with quantal variance ($CV_Q = 0.07 \pm 0.02$) and no constraints on the amplitude probabilities. The details are provided in Table 3.

An example with a significant number of failures (P_0) and a positive skew, which is indicative of a lower release probability, is shown in Fig. 7. The PDF was formed from 521 EPSCs based on a kernel size of 0.19 pA. The average size of the EPSC was -7.7 ± 5.0 pA and $\sigma_n = 0.74$ pA. Similar to the case above, the PDF was identified as multimodal with $K = 10$ and with all unimodal hypothesis rejectable at $P_{MC} < 0.004$. The best fitting model was a quantal model ($Q = -2.0 \pm 0.2$ pA) but without quantal variance ($P_\chi = 0.88$). We were unable

to identify a binomial release process ($P_{MC} \ll 0.004$), and therefore, were left with no constraints on the 10 amplitude probabilities. Again, this finding can easily be reconciled based on a qualitative consideration: as in the example before, the PDF has more failures than would be predicted from a binomial process.

Of the 28 connections investigated, 19 PDFs were sufficiently multimodal (68%) to warrant a full analysis. A unimodal hypothesis could not be ruled out for the remaining nine connections. For this subset, the average R_{in} and R_A were 260 ± 102 and 13 ± 5 M Ω , respectively. The average sample size making up the PDFs was 455 ± 129 , and σ_n was 0.9 ± 0.2 (Table 3). For all PDFs, the modes were equally separated and therefore quantized. The average quantal size was -2.8 ± 0.7 pA. The amplitude distributions of seven connections (32%) required quantal variance; for these cases, the average CV_Q was 0.21 ± 0.12 (intrasite variability). The PDFs of the 19 EPSCs ranged from those with negative skew with few failures (indicative of a high average P) to those with a positive skew and a significant number of failures (low average P). Only four amplitude distributions could be fitted with a binomial model of transmitter release (average $P = 0.41 \pm 0.05$; 18% of total sample, these four EPSCs are significantly smaller (-3.2 ± 1.8 vs. -10.7 ± 3.7 pA, $P_t = 0.001$), and the PDFs are made up of fewer components (4 ± 1 vs. 7 ± 2 , $P_t = 0.002$), indicating that these four examples represent a distinct group with few modes. The details of all connections analyzed are given in Table 3.

Two parameters that do not rely on any estimation based on quantal analysis, namely failure rate and the average size of the EPSC, were examined to see if they were correlated. This was, in fact the case ($r = 0.82$, $P_r < 10^{-4}$; Fig. 8A). Testing whether the quantal parameters obtained were consistent with this finding, we examined whether quantal content was still correlated with the average EPSC. This was the case ($r = 0.88$, $P_r < 10^{-6}$; Fig. 8B) and supports our argument that the quantal

TABLE 3. *Quantal properties of individual connections*

Cell Type	N	σ_n , pA	E , pA	R_A , M Ω	R_{in} , M Ω	RT , ms	HW , ms	P_0	Model	K	Q , pA	CV_Q	m	P
SS-SS	573	1.34	-13.5 ± 7.3	8	107	1.4	4.0	0.12 ± 0.02	QuQv	7	-3.7 ± 0.3	0.19 ± 0.07	3.6 ± 0.6	
SS-SS	404	1.13	-10.8 ± 4.3	6	240	1.8	6.2	0.05 ± 0.02	Qu	8	-3.1 ± 0.3		3.5 ± 0.6	
SS-SP*	463	0.98	-16.6 ± 7.2	9	165	1.2	3.6	0.06 ± 0.01	QuQv	9	-3.6 ± 0.1	0.07 ± 0.02	4.7 ± 0.4	
SS-SP	627	0.64	-11.9 ± 4.7	19	205	1.7	7.8	0.00 ± 0.00	QuQv	6	-3.9 ± 0.1	0.22 ± 0.02	3.0 ± 0.3	
SS-SP	407	0.71	-1.6 ± 1.9	16	256	1.2	4.0	0.36 ± 0.09	BQv	3	-2.3 ± 0.3	0.36 ± 0.21	0.7 ± 0.2	0.39 ± 0.07
SP-SP	446	0.69	-10.7 ± 3.8	4	307	1.9	9.0	0.04 ± 0.02	Qu	8	-2.0 ± 0.2		5.2 ± 0.9	
SP-SP	250	0.80	-9.6 ± 4.0	20	162	1.5	5.0	0.05 ± 0.02	Qu	7	-2.6 ± 0.2		3.8 ± 0.5	
SP-SP†	521	0.74	-7.7 ± 5.0	15	214	1.7	7.5	0.13 ± 0.02	Qu	10	-2.0 ± 0.2		3.8 ± 0.6	
SP-SP	477	1.14	-10.3 ± 4.6	10	554	1.6	6.8	0.08 ± 0.02	Qu	7	-2.7 ± 0.2		3.8 ± 0.6	
SP-SP	401	0.81	-10.2 ± 3.3	10	364	1.8	6.2	0.03 ± 0.01	Qu	7	-2.4 ± 0.1		4.3 ± 0.4	
SP-SP	470	0.92	-4.0 ± 2.3	16	403	1.7	5.1	0.17 ± 0.03	BQv	4	-2.2 ± 0.1	0.38 ± 0.09	1.8 ± 0.2	0.44 ± 0.03
SP-SP	253	0.90	-5.4 ± 4.4	8	213	1.0	4.1	0.29 ± 0.03	Qu	5	-3.1 ± 0.2		1.8 ± 0.3	
SP-SP	309	0.87	-13.2 ± 5.6	14	216	1.1	3.1	0.07 ± 0.02	Qu	9	-2.5 ± 0.3		5.4 ± 1.0	
SP-SP	271	0.97	-15.5 ± 5.4	17	173	1.5	8.0	0.04 ± 0.02	Qu	8	-2.7 ± 0.3		5.8 ± 1.1	
SP-SP	747	0.89	-12.4 ± 7.2	14	265	1.5	4.9	0.19 ± 0.02	QuQv	9	-2.8 ± 0.2	0.09 ± 0.07	4.4 ± 0.5	
SP-SS	498	0.75	-10.2 ± 6.8	10	345	1.1	3.7	0.18 ± 0.02	QuQv	6	-4.2 ± 0.2	0.19 ± 0.04	2.4 ± 0.3	
SP-SS	450	0.90	-5.3 ± 4.6	16	267	1.8	5.4	0.35 ± 0.02	B	6	-2.7 ± 0.1		2.0 ± 0.2	0.47 ± 0.02
SP-SS	577	0.76	-1.9 ± 1.7	17	254	1.9	4.5	0.42 ± 0.04	B	3	-1.9 ± 0.1		1.0 ± 0.1	0.35 ± 0.03
SP-SS	498	0.79	-2.2 ± 1.8	14	235	1.6	9.1	0.40 ± 0.04	Qu	4	-2.2 ± 0.1		1.0 ± 0.1	
Mean	455 ± 129	0.9 ± 0.2	-9.1 ± 4.6	13 ± 5	260 ± 102	1.5 ± 0.3	5.7 ± 1.9	0.16 ± 0.14			-2.8 ± 0.7	0.21 ± 0.12	3.3 ± 1.6	0.41 ± 0.05

Values are means \pm SD. SS, spiny stellate; SP, star pyramid; N , number of records used to construct the PDF; σ_n , SD of the noise; \bar{E} , mean peak amplitude; R_A , access resistance; R_{in} , input resistance; RT , 10–90% rise time of EPSC; HW , half-width; Model, type of model that best fits the PDF; Qu, unconstrained quantal model; QuQv, unconstrained quantal model with variance; B, binomial model; BQv, binomial model with variance; K , number of amplitude components; Q , quantal size; CV_Q , coefficient of variation of quantal current; m , quantal content; P_0 , probability of failures, and P , release probability. Examples shown in *Figs. 6 and †7, respectively.

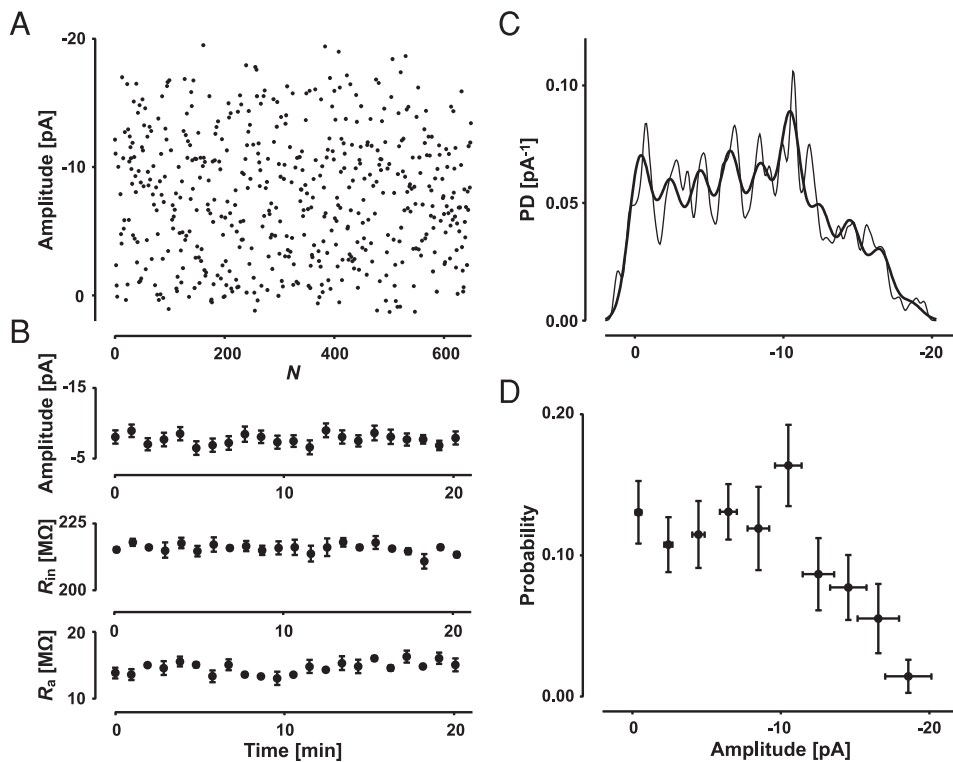


FIG. 7. Example of quantal analysis of a connection with lower release probability. *A*: maximal amplitude of 521 individual EPSCs recorded at 0.5 Hz in a SP–SP pair (Table 3, †). *B–D*: as in Fig. 6, except that the optimal fit is a quantal model with no restraints placed on the release process and no requirement for quantal variance.

parameters obtained are consistent with two estimation-independent measures. Further exploration showed that the average current at each synapse is correlated with the number of components identified in the distribution ($r = -0.80$, $P_r < 10^{-4}$; Fig. 8C). This finding indicates that the number of components (i.e., the number of release sites; see DISCUSSION where we show that in general P is high and hence K does not underestimate number of active sites) determines the size of the EPSC. If that is the case, the failure rate should decrease as K becomes larger. This was found to be true ($r = -0.71$, $P_r < 10^{-4}$; Fig. 8D). In a next step, we checked whether the quantal size had any relationship with K and found that they were independent of each other ($r = -0.16$, $P_r = 0.52$; Fig. 8E). Since this is the case, the quantal content had to be correlated with K , which was found to hold true ($r = -0.88$, $P_r < 10^{-6}$; Fig. 8F). This indicates that each of the synapses in the connection contributes, on average, the same amount to the overall current.

Cell-specific differences

Given that there are two excitatory neuronal types within layer IV, we investigated whether there were any differences in synaptic strength based on different pre- or postsynaptic cell types. Significant differences were observed in m and Q . When the presynaptic neuron was a SS cell, Q was larger than that for SP cells (-3.3 ± 0.7 vs. -2.6 ± 0.6 pA, $P_t < 0.05$; Table 4), irrespective of the postsynaptic cell type. Conversely, when the postsynaptic neuron was a SS cell, m was smaller than when the postsynaptic neuron was a SP cell (2.3 ± 1.1 vs. 3.7 ± 1.5 , $P_t < 0.05$; Table 4), irrespective of the type of presynaptic neuron.

We found a difference in synaptic efficacy for the two groups formed by homo- and heteronymous connections. The

quantal size was not significantly different (mean: -2.7 ± 0.5 vs. -3.0 ± 0.9 pA; Table 4); however, the quantal content (3.9 ± 1.2 cf. 2.2 ± 1.4 , $P_t < 0.01$) and number of components ($K = 7.4 \pm 1.7$ vs. 5.3 ± 2.1 , $P_t < 0.05$) were both greater for homo- than for heteronymous connections.

DISCUSSION

Despite the fact that SS and SP cells have markedly different morphological characteristics, the two excitatory neuronal types of layer IV could hardly be distinguished by their intrinsic properties. In fact, they were surprisingly homogenous in regard to the basic electrophysiological properties. However, synaptic properties showed significant differences between the various types of connection.

Properties of excitatory synapses in layer IV

Within excitatory-excitatory connections, we determined that not all pathways were of equal strength. Homonymous connections had a greater synaptic efficacy than heteronymous connections. The mechanism is a higher release probability as evidenced by fewer failures, larger paired-pulse depression, and a more negative skew than for heteronymous pairs (Table 1). These findings were also supported by quantal analysis: the homonymous connections had a significantly greater quantal content, which was partly accounted for by a greater number of modes in the PDFs (potentially indicating a larger number of release sites). In addition, there was evidence for target specificity in synaptic efficacy: the quantal content was larger when the postsynaptic neuron was an SP cell than when it was an SS cell, irrespective of the presynaptic cell type.

Comparison of the various types of connections did not show any differences in the postsynaptic properties of synaptic

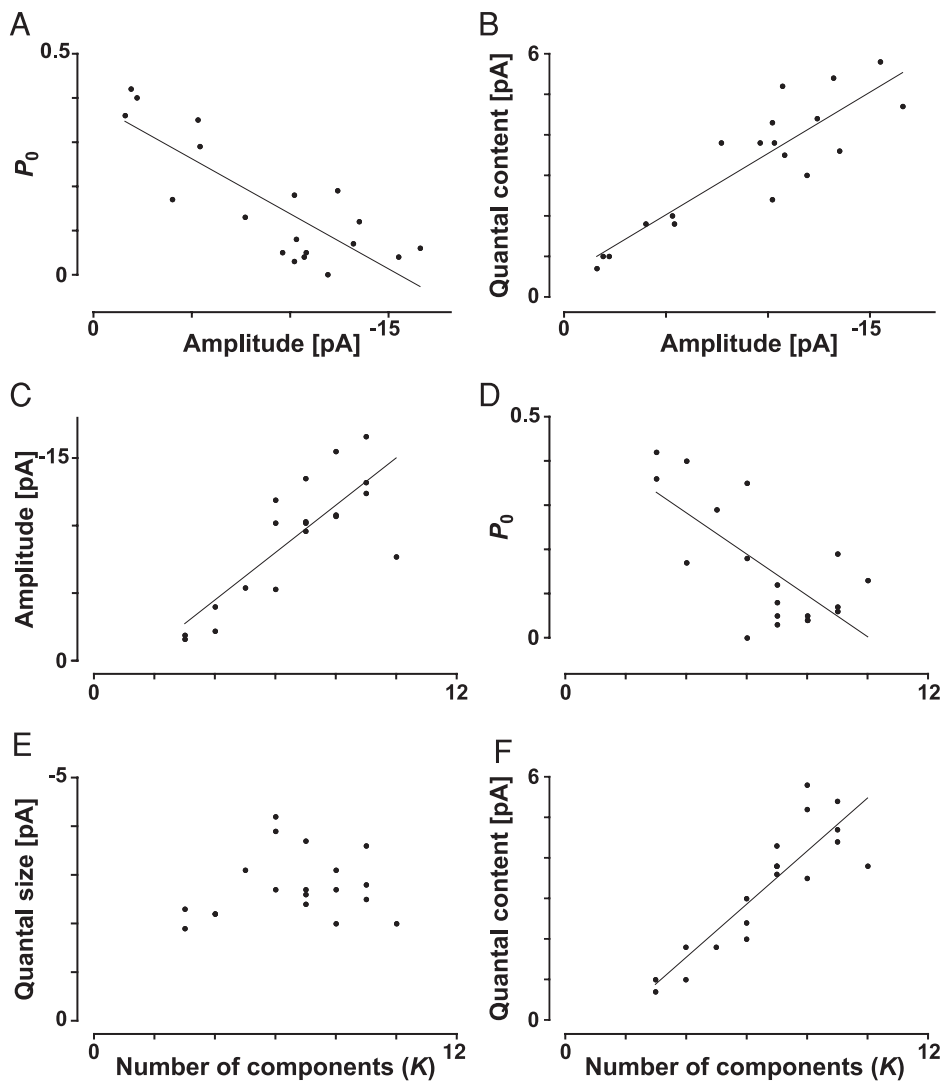


FIG. 8. Correlations between synaptic parameters. *A*: estimation-independent parameters (failure rate and average amplitude) are correlated ($r = -0.82$, $P_r < 10^{-4}$, $n = 19$). Line indicates the correlation obtained. *B*: correlation between quantal content and average amplitude ($r = -0.88$, $P_r < 10^{-6}$), indicating that the results of quantal analysis are consistent with estimation-independent parameters. *C*: quantal size (Q) is correlated with the number of components (K , $r = -0.80$, $P_r < 10^{-4}$). *D*: with a larger K , a smaller failure rate (P_0) would be expected ($r = -0.71$, $P_r < 0.001$). *E*: Q and K are independent of each other ($r = -0.16$, $P_r = 0.52$). *F*: quantal content is also correlated with K ($r = -0.88$, $P_r < 10^{-6}$). These correlations indicate that each of the synapses contributes, on average, the same amount to the overall current.

transmission (i.e., quantal size). However, we could show that some specificity in this parameter did occur based on the type of presynaptic neuron: the quantal size was larger when the presynaptic neuron was an SS cell than when it was an SP cell.

TABLE 4. Summary of quantal characteristics of types of connections

Cell Type	N	K	Q , pA	m
SS-SS	2	7.5 ± 0.7	-3.4 ± 0.5	3.6 ± 0.1
SS-SP	3	6.0 ± 3.0	-3.3 ± 0.9	2.9 ± 2.0
SP-SP	10	7.4 ± 1.8	-2.5 ± 0.4	4.0 ± 1.4
SP-SS	4	4.8 ± 1.5	-2.8 ± 1.0	1.6 ± 0.7
Homonymous	12	7.4 ± 1.7	-2.7 ± 0.5	3.9 ± 1.2
Heteronymous	7	$5.3 \pm 2.1^*$	-3.0 ± 0.9	$2.2 \pm 1.4^\dagger$
Presynaptic SS	5	6.6 ± 2.3	-3.3 ± 0.7	3.2 ± 1.5
Presynaptic SP	14	6.6 ± 2.1	$-2.6 \pm 0.6^*$	3.3 ± 1.6
Postsynaptic SS	6	5.7 ± 1.9	-3.0 ± 0.9	2.3 ± 1.1
Postsynaptic SP	13	7.1 ± 2.1	-2.7 ± 0.6	$3.7 \pm 1.5^*$
All	19	6.6 ± 2.1	-2.8 ± 0.7	3.3 ± 1.6

Values are means \pm SD. Statistically different from the preceding value at $*P_r < 0.05$ and at $^\dagger P_r < 0.01$. SS, spiny stellate cell; SP, star pyramid; N_Q , Number of connections for which a full quantal analysis was performed; K , average number of components in the PDF; Q , average quantal size; m , quantal content.

Short-term synaptic dynamics

All connections in this study showed short-term synaptic depression (Abbott et al. 1997; Tsodyks and Markram 1997). However, the type of depression varied from purely release-dependent to completely release-independent (Fig. 3). Release-independent depression (RID) has previously been described in neocortex (Thomson and Bannister 1999). Potential mechanisms are discussed in more detail in Fuhrmann et al. (2004). The fact that we found the same properties for RID in layer IV as in layer V cells suggests that this property of depression might be a general feature at many synapses.

When examining the properties of depression (Table 2), target specificity was evident. RID was significantly more pronounced when the postsynaptic neuron was an SP cell than when it was an SS cell, irrespective of the presynaptic cell type. There was also a strong tendency for presynaptic SP cells to exhibit less RID (Table 2). The combined effect of these pre- and postsynaptic differences was that the two types of heteronymous connections showed the most striking differences in the type of depression. SS-SP connections showed nearly complete RID, whereas the dominant form of depression in SP-SS was release-dependent.

The data presented here differ from the study of layer IV connections by Petersen (2002), where it was found that synaptic depression was release-dependent. This discrepancy could be related to a number of factors. First, Petersen (2002) used similar techniques to Feldmeyer et al. (1999) and similarly found reliable connections. We have shown that there is a relationship between release probability and release-dependent depression, so it is not surprising that Petersen (2002) found more release-dependence than we did. Furthermore, it is not clear from the data presented in that paper whether the depression was purely release-dependent or just showed some correlation between the amplitude of the first and second EPSP. Most of our connections showed some degree of release-dependence, but it was not pure release-dependence.

Control of synaptic efficacy by presynaptic V_m

A subset of connections where the presynaptic neuron was an SP cell showed a novel form of modification of synaptic strength (Fig. 5). The synaptic strength decreased with increasing depolarization. This is unlikely to be solely due to increasing inactivation of Na^+ channels, because subtle changes in synaptic strength could also be seen at $V_m < -65$ mV and with only small (5 mV) changes in voltage, where Na^+ -channel inactivation won't contribute significantly. However, the almost complete absence of transmission at a membrane potential of -50 mV could well be explained by effects on Na^+ channels. Activation/inactivation of other voltage-dependent channels (i.e., Ca^{2+} channels) may well underlie the voltage-sensitivity of synaptic transmission at these connections. However, it is unlikely to be a direct effect because there is a significant delay after changing the membrane potential before any effect is observed. This indicates that a slower process (such as a signaling cascade) may be involved. A somewhat similar change in synaptic strength with changes in V_m has been observed in the hippocampus (Debanne et al. 1997; Saviane et al. 2003). However, in their case, the change in synaptic efficacy was the opposite of that observed in our study and occurred without delay. The authors argued that the phenomenon is due to branch point failure due to activation of I_A or I_D . It seems likely that the effect observed in our experiments occurs at the terminals rather than in the axon since there is an interaction between changes in V_m and R_D .

An open question is how much of the polarization is seen at the terminal. Given that the terminals occur on average $70 \mu\text{m}$ distal from the soma (Feldmeyer et al. 1999), that the length of the axon is $\geq 70 \mu\text{m}$ (more realistically around $200 \mu\text{m}$), that each terminal emanates from a cable without sealed ends, and that the diameter of the axon is $< 1 \mu\text{m}$, we can estimate that the length constant is of the order of $700 \mu\text{m}$ (using parameter values from Bannister et al. 2002). Under those conditions, the voltage decrement at the terminal is of the order of $< 10\%$ to maximally 27% . Given very conservative estimates in regard to axon diameter and lack of myelination, most of the polarization at the soma is actually experienced at the terminal. Thus relief of steady-state Ca^{2+} channel inactivation might play a role in the range of potentials experienced (Patil et al. 1998; Villarroya et al. 1999). However, this would not explain why we observed this phenomenon in only a subset of connections and, notably, only for one presynaptic cell type (SP).

The fact that there are significant changes in synaptic efficacy with only small changes in V_m would indicate that the functional role could be very significant, e.g., when V_m changes due to synaptic noise, during barrages of subthreshold synaptic activity, or due to the effect of neuromodulators. The changes in R_D with changing presynaptic V_m are not just a result of changes in release probability. Between -75 and -85 mV, there are no significant changes in the skew of the amplitude distribution; however, R_D changes markedly within this range. The detailed issues underlying this process are left for future investigation.

Reliability of transmission

Recently, it has been stated directly (Feldmeyer and Sakmann 2000; Feldmeyer et al. 1999; Petersen 2002) and indirectly (Tarczy-Hornoch et al. 1999) that the synaptic efficacy and reliability of excitatory-excitatory connections within layer IV is high. We found a wide range of failure rates, paired-pulse depression, and skews within connections in layer IV. We suggest that synaptic efficacy in this layer is variable; at most connections tested, there is a significant proportion of failures to release transmitter. Based on these observations, release probability is on average < 0.5 . Our data are in agreement with those of Gil et al. (1999), where in mouse somatosensory cortex, an upper limit for release probability of about 0.6 can be inferred.

The studies of Feldmeyer and colleagues (Feldmeyer and Sakmann 2000; Feldmeyer et al. 1999) are directly comparable with our study (although they used slightly younger animals). They found that excitatory-excitatory connections within layer IV were highly reliable (low failure rate). They did not observe differences in synaptic strength between the various types of connection based on excitatory postsynaptic potential (EPSP) amplitude or failure rate. We think that the difference between their results and ours may be because synaptic responses were measured in voltage rather than current clamp. The improved signal-to-noise ratio in voltage-clamp (see Fig. 2) may be a limiting factor for identifying small amplitude connections. We therefore argue that we have been able to record from a slightly less biased sample. This idea is supported by the fact that CV and failure rate recorded in our experiments were significantly higher (and covered a larger range). Another potential technical difference is that most of our experiments were performed using parasagittal rather than thalamocortical slices and that we did not use loose patches to search for connections. However, we did a number of experiments ($n = 12$) in thalamocortical slices to investigate the possibility of a systematic difference in connection strength between the two slicing procedures. We could not find any differences; in fact, some of our smallest amplitude connections are from thalamocortical slices (Fig. 2).

In contrast, in cat visual cortex, Tarczy-Hornoch et al. (1999) found that excitatory-excitatory connections had a uniformly high P . The discrepancy with our results may be due to differences in age (older animals in their study), species, cortical area investigated, or the method used for estimating P . Their method was based on the assumption of binomial release statistics and required estimates for both quantal size and number of release sites, which were not measured. In only four of our recordings could we identify a binomial process, for

which, on average, P was <0.5 (also supported by the average skew of 0.3 ± 1.0).

Most of the models identified were unconstrained in amplitude probability, and only four could be fitted with a binomial model of transmitter release (Table 3). These four require special mention in that significantly fewer modes (4 ± 1 vs. 7 ± 2) were present, indicating fewer release sites. It is not surprising that, for these recordings, the binomial release model could not be rejected since only a few modes were present in the PDFs, leaving little room for deviation from binomial statistics together with the inherent bias of the analysis toward the latter. One reason for the inability to fit binomial models to the other connections was that, even at junctions with relatively high P , there were still more failures to release transmitter than predicted by a classical model. These failures are unlikely to be caused by the mechanism responsible for RID, since the stimulus intervals between trials were more than three times longer than the recovery time constants.

Estimates of quantal size

The average quantal size was -2.8 ± 0.6 pA as measured at the soma. This number is about one-third of that reported by Gil et al. (1999) for synapses in mouse barrel cortex obtained from stimulating extracellularly. Given that these authors used QX-314 to increase input resistance significantly, which improves space-clamp conditions, a bigger quantal size is expected. Furthermore, since their presynaptic terminals remained unidentified (thalamo- and intracortical) and it appears that quantal size is dependent on the particular synapse investigated (this study), direct comparisons are not justified. An even smaller quantal size can be estimated from the data of Silver et al. (2003) at layer IV to II/III synapses.

Quantal analysis and estimated release sites

If P in a binomial process is neither too small nor too big ($0.2 < P < 0.8$) and only a few release sites ($n < 5$) are involved in generating the EPSC, the number of components, K , detected in a PDF is $n + 1$, which corresponds to 5.6 ± 2.1 in these cells (Tables 1 and 2). This number is somewhat larger than, but not very different from, the 3.4 ± 1.0 morphologically determined by Feldmeyer et al. (1999). The discrepancy could result from multivesicular release from one site (Auger et al. 1998), multiple release sites within one terminal (e.g., Sorra and Harris 1993), uncertainty within the reconstruction, partial filling of the axonal arbour, and synapse identification at the light microscopic level. Even if synaptic terminals and release sites were positively identified with electron microscopy (EM), there is still uncertainty in regard to functionality.

Data displayed in Fig. 8 served as a test for the reliability of the quantal parameters. If the average EPSC was correlated with the number of components, and hence, the number of release sites, the failures should be negatively correlated with K , which they were. The failures could be estimated directly from the PDFs without much bias, whereas K is determined from the number of noise modes in the distribution and relies on density estimation. Failures versus average EPSC current, two estimation-independent parameters, and quantal current versus EPSC current were still correlated and highly signifi-

cant. Both correlations together indicate that the quantal parameters were estimated reliably.

We believe that the method of quantal analysis used here produces an accurate estimate of the number of release sites even in the absence of morphological evidence, because it provides results consistent with density estimation-independent measures of synaptic parameters. This statement is further supported by a recent study where synaptic fluctuations matched the number of synapses subsequently identified by EM (Buhl et al. 1997).

Comparison with Schaffer collateral synapses on CA1 pyramidal cells

This is the first study in which a full quantal analysis, as described in Stricker et al. (1994), has been rigorously applied to recordings between pairs of cells as compared with minimal stimulation (Stricker et al. 1996). In addition, it allows comparisons of transmission characteristics between cortical and hippocampal synapses. Surprisingly, in cortex, 68% of connections studied (compared with 42% in hippocampus; Stricker et al. 1996) could be well described by a quantal process, not requiring much variability. The higher rate of successful analysis might reflect more homogeneous conditions in regard to release characteristics and location on the postsynaptic neuron, i.e., recordings from a cell pair rather than from an unknown number of fibers. It is unlikely that the success rate reflected a reduced sensitivity of testing even though two of the unimodal hypotheses (cubic transform and gamma distribution) can only describe positive skewness. In all cases with negative skew, the Weibull distribution was rejectable, most often with $P_{MC} < 0.004$.

Given that the number of quantal analyses, σ_n , the number of EPSCs in each density, and even the number of modes in the distributions are the same in this study (Table 3) and in Table 3 in Stricker et al. (1996), a comparison of the two data sets is possible. In particular, Q was on average 2.8 ± 0.6 pA, slightly bigger and with smaller variability than at CA3–CA1 synapses. Again, it might reflect a more homogeneous synapse population and electrotonic characteristics. The resolution of the quantum in terms of signal-to-noise ratio (Q/σ_n) was the same (3.1 ± 1.0 , $P_t = 0.6$), and the variability (intrasite) as indicated by CV_Q , if required, was small (0.21 ± 0.12), identical to the previous finding. Two properties are different in layer IV. First, the apparent EPSC kinetics in cortex are about twice as fast as in hippocampus (both in rise-time and half-width). This might be caused by R_{in} , which is about three times higher than in CA1 pyramidal cells, and the effect this has on the properties of the voltage clamp. Lacking a detailed passive model of an SS and an SP cell, we have not been able to study these effects on the kinetic properties. Second, the most striking difference is in quantal content between excitatory cell pairs (3.3 ± 1.6 vs. 1.8 ± 0.8 , $P_t < 0.0005$). Given that the number of release sites in both studies is comparable, this observation can only be explained by a bigger P , consistent with few failures, paired-pulse depression, and a more negative skew.

Number of release sites determines the size of the EPSC

In terms of functional importance, we found that the size of the EPSC is simply determined by the number of release sites,

and therefore, each release site is, on average, contributing the same amount of current to the unitary/single-fiber EPSC ($P_r < 0.0001$). A similar finding (close to significance) was obtained earlier (Feldmeyer et al. 1999). It implies that, independent of the location, the current is roughly identical. Such scenarios have been reported previously (Jack et al. 1981; Magee and Cook 2000; Stricker et al. 1996).

If all synapses are the same when seen at the soma in voltage clamp, any functional differences must be due to postsynaptic processing (i.e., active dendrites). At these connections and under our stimulus conditions, the synaptic efficacy might be homogeneous. However, this finding does not imply that there are no differences in short-term dynamics.

Evidence for two separate pathways

The finding that there were hardly any differences in intrinsic properties between the two types of excitatory neuron was surprising, given that the morphological differences between the two cell types can be very pronounced (see Fig. 1). Since morphological characteristics affect the intrinsic properties and firing characteristics of a neuron (Connors and Regehr 1996; Kim and Connors 1993; Mainen and Sejnowski 1996; van Pelt and Schierwagen 1994), and SS cells have apparently lost an initial apical dendrite during development (Amitai and Connors 1995; Peinado and Katz 1990; Vercelli et al. 1992), the question arises as to what are the mechanisms that, despite different dendritic structure, tune both neurons to an indistinguishable electrical behavior.

With their different dendritic structure, both cell types will likely sample different synaptic inputs. This has been shown to be true of intracortical connections (Schubert et al. 2003). It is not known whether SS and SP cells receive selective input from different thalamocortical connections or whether they have a selective axonal targeting. The target specificity we observed might support this idea. These factors, which might lead to an anatomical separation of inputs, together with the differences between homo- and heteronymous pairs in local connectivity, efficacy, and dynamics, might sufficiently alter the functional properties within a network such that two separate pathways could emerge.

View of the layer IV local circuit

The important question is how these detailed and subtle differences between different types of connection might play a role within the local circuit and in processing of sensory information. The behavior of the local circuit may be modified by "up-states" and "down-states," as described in cortical neurons recorded in vivo (Anderson et al. 2000; Brecht and Sakmann 2002; Brecht et al. 2003). In the "down-state," where V_m may be 30 mV more hyperpolarized than in the "up-state," the synaptic efficacy from presynaptic SP cells is much higher, and thus, information between the cell types will be more effectively transmitted. As excitation (and depolarization) increases, the strength of the connections from SP cells decreases, and in addition, since the depression from SP to SS cells is largely release-dependent, the effect is accentuated. These two factors would then ensure that, during the "up-state," the two cell types within layer IV work within networks of preferentially homonymous cells. Most connections within

layer IV show mainly release-independent depression, which would allow them to code presynaptic activity even at high-frequency (see Fuhrmann et al. 2004).

In conclusion, we suggest that the local circuit behavior in layer IV of rat somatosensory cortex is modified according to the state of excitation. During high-frequency activity and/or depolarization, there are two preferential local excitatory circuits, which correspond to circuits within the two morphologically distinct excitatory cell types: SS and SP. These two circuit types are only weakly connected with each other. However, during periods of lower activity or during hyperpolarization, these two circuits interact due to the increased efficacy of the connection emanating from SP cells.

ACKNOWLEDGMENTS

We thank Dr. S. J. Redman for comments on the manuscript.

GRANTS

This work was supported by Swiss National Science Foundation (5002-52085, 5002-57809, 31-59309), Bonizzi-Theler Foundation, Zürich, and Jubiläumsstiftung der Schweizerischen Mobiliar Gesellschaft, Bern, Switzerland.

REFERENCES

- Abbott LF, Varela JA, Sen K, and Nelson SB. Synaptic depression and cortical gain control. *Science* 275: 220–224, 1997.
- Agmon A and Connors BW. Thalamocortical responses of mouse somatosensory (barrel) cortex in vitro. *Neuroscience* 41: 365–379, 1991.
- Amitai Y and Connors BW. Intrinsic physiology and morphology of single neurons in neocortex. In: *The Barrel Cortex of Rodents*, edited by Jones EG and Diamond IT. New York: Plenum Press, 1995, p. 299–331.
- Anderson JS, Lampl I, Reichova I, Carandini M, and Ferster D. Stimulus dependence of two-state fluctuations of membrane potential in cat visual cortex. *Nat Neurosci* 3: 617–621, 2000.
- Auger C, Kondo S, and Marty A. Multivesicular release at single functional synaptic sites in cerebellar stellate and basket cells. *J Neurosci* 18: 4532–4547, 1998.
- Bannister NJ, Nelson JC, and Jack JJB. Excitatory inputs to spiny cells in layers 4 and 6 of cat striate cortex. *Phil Trans R Soc Lond B* 357: 1793–1808, 2002.
- Brecht M, Roth A, and Sakmann B. Dynamic receptive fields of reconstructed pyramidal cells in layers 3 and 2 of rat somatosensory barrel cortex. *J Physiol* 553: 234–265, 2003.
- Brecht M and Sakmann B. Dynamic representation of whisker deflection by postsynaptic potentials in morphologically reconstructed spiny stellate and pyramidal cells in the barrels and septa of layer 4 in rat somatosensory cortex. *J Physiol* 543: 49–70, 2002.
- Buhl EH, Tamás G, Szilágyi T, Stricker C, Paulsen O, and Somogyi P. Effect, number and location of synapses made by single pyramidal cells onto aspiny interneurons of cat visual cortex. *J Physiol* 500: 689–713, 1997.
- Connors BW and Regehr WG. Neuronal firing: does function follow form? *Curr Biol* 6: 1560–1562, 1996.
- Debanne D, Guérineau NC, Gähwiler BH, and Thompson SM. Action-potential propagation gated by an axonal I_A -like K^+ conductance in hippocampus. *Nature* 389: 286–289, 1997.
- Dotz H-U and Zieglgänsberger W. Visualizing unstained neurons in living brain slices by infrared DIC-videomicroscopy. *Brain Res* 537: 333–336, 1990.
- Elston GN, Pow DV, and Calford MB. Neuronal composition and morphology in layer IV of two vibrissal barrel subfields of rat cortex. *Cereb Cortex* 7: 422–431, 1997.
- Feldmeyer D, Egger V, Lübke J, and Sakmann B. Reliable synaptic connections between pairs of excitatory layer 4 neurones within a single 'barrel' of developing rat somatosensory cortex. *J Physiol* 521: 169–190, 1999.
- Feldmeyer D and Sakmann B. Synaptic efficacy and reliability of excitatory connections between the principal neurones of the input (layer 4) and output layer (layer 5) of the neocortex. *J Physiol* 525: 31–39, 2000.
- Fuhrmann G, Cowan AI, Segev I, Tsodyks MV, and Stricker C. Multiple mechanisms govern synaptic dynamics at neocortical synapses. *J Physiol* 557: 415–438, 2004.

- Gil Z, Connors BW, and Amitai Y.** Efficacy of thalamocortical and intracortical synaptic connections: Quanta, innervation, and reliability. *Neuron* 23: 385–397, 1999.
- Horikawa K and Armstrong WE.** A versatile means of intracellular labeling: Injection of biocytin and its detection with avidin conjugates. *J Neurosci Methods* 25: 1–11, 1988.
- Jack JJB, Redman SJ, and Wong K.** The components of synaptic potentials evoked in cat spinal motoneurons by impulses in single group Ia afferents. *J Physiol* 321: 65–96, 1981.
- Keller A.** Synaptic organization of the barrel cortex. In: *The Barrel Cortex of Rodents*, edited by Jones EG and Diamond IT. New York: Plenum Press, 1995, p. 221–262.
- Kim HG and Connors BW.** Apical dendrites of the neocortex: correlation between sodium- and calcium-dependent spiking and pyramidal cell morphology. *J Neurosci* 13: 5301–5311, 1993.
- Lübke J, Egger V, Sakmann B, and Feldmeyer D.** Columnar organization of dendrites and axons of single and synaptically coupled excitatory spiny neurons in layer 4 of the rat barrel cortex. *J Neurosci* 20: 5300–5311, 2000.
- Magee JC and Cook EP.** Somatic EPSP amplitude is independent of synapse location in hippocampal pyramidal neurons. *Nat Neurosci* 3: 895–903, 2000.
- Mainen ZF and Sejnowski TJ.** Influence of dendritic structure on firing pattern in model neocortical neurons. *Nature* 382: 363–366, 1996.
- Matveev V and Wang X-J.** Implications of all-or none synaptic transmission and short-term depression beyond vesicle depletion: a computational study. *J Neurosci* 20: 1575–1588, 2000.
- Patil PG, Brody DL, and Yue DT.** Preferential closed-state inactivation of neuronal calcium channels. *Neuron* 20: 1027–1038, 1998.
- Peinado A and Katz LC.** Development of cortical spiny stellate cells: retraction of a transient apical dendrite. *Soc Neurosci Abstr* 16: 1127, 1990.
- Peters A and Kara DA.** The neuronal composition of area 17 of rat visual cortex. I. The pyramidal cells. *J Comp Neurol* 234: 218–241, 1985.
- Petersen CCH.** Short-term dynamics of synaptic transmission within the excitatory neuronal network of rat layer 4 barrel cortex. *J Neurophysiol* 87: 2904–2914, 2002.
- Saviane C, Mohajerani MH, and Cherubini E.** An I_P -like current that is downregulated by Ca^{2+} modulates information coding at CA3-CA3 synapses in the rat hippocampus. *J Physiol* 552: 513–524, 2003.
- Scheuss V, Schneggenburger R, and Neher E.** Separation of presynaptic and postsynaptic contributions to depression by covariance analysis of successive EPSCs at the calyx of Held synapse. *J Neurosci* 22: 728–739, 2002.
- Schubert D, Kötter R, Zilles K, Luhmann HJ, and Staiger JF.** Cell type-specific circuits of cortical layer IV spiny neurons. *J Neurosci* 23: 2961–2970, 2003.
- Silver RA, Lübke J, Sakmann B, and Feldmeyer D.** High-probability unquantal transmission at excitatory synapses in barrel cortex. *Science* 302: 1981–1984, 2003.
- Silverman BW.** *Density Estimation for Statistics and Data Analysis*. London: Chapman and Hall, 1986.
- Simkus CRL and Stricker C.** Analysis of mEPSCs recorded in layer II neurons of rat barrel cortex. *J Physiol* 545: 509–520, 2002.
- Simons DJ and Woolsey TA.** Morphology of Golgi-Cox-impregnated barrel neurons in rat SmI cortex. *J Comp Neurol* 230: 119–132, 1984.
- Sorra KE and Harris KM.** Occurrence of three-dimensional structure of multiple synapses between individual radiatum axons and their target pyramidal cells in hippocampal area CA1. *J Neurosci* 13: 3736–3748, 1993.
- Stricker C, Daley D, and Redman SJ.** Statistical analysis of synaptic transmission: model discrimination and confidence limits. *Biophys J* 67: 532–547, 1994.
- Stricker C, Field AC, and Redman SJ.** Statistical analysis of amplitude fluctuations in EPSCs evoked in rat CA1 pyramidal neurons in vitro. *J Physiol* 490: 419–441, 1996.
- Tarczy-Hornoch K, Martin KAC, Stratford KJ, and Jack JJB.** Intracortical excitation of spiny neurons in layer 4 of cat striate cortex in vitro. *Cereb Cortex* 9: 833–843, 1999.
- Thomson AM and Bannister AP.** Release-independent depression at pyramidal inputs onto specific cell targets: Dual recordings in slices of rat cortex. *J Physiol* 519: 57–70, 1999.
- Tsodyks MV and Markram H.** The neural code between neocortical pyramidal neurons depends on neurotransmitter release probability. *Proc Natl Acad Sci USA* 94: 719–723, 1997.
- van Pelt J and Schierwagen A.** Electrotonic properties of passive dendritic trees—effect of dendritic topology. *Prog Brain Res* 102: 127–149, 1994.
- Vercelli A, Assal F, and Innocenti GM.** Emergence of callosally projecting neurons with stellate morphology in the visual cortex of the kitten. *Exp Brain Res* 90: 346–358, 1992.
- Villarroya M, Olivares R, Ruíz A, Cano-Abad MF, de Pascual R, Lomax RB, López MG, Mayorgas I, Gandía L, and García AG.** Voltage inactivation of Ca^{2+} entry and secretion associated with N- and P/Q-type but not L-type Ca^{2+} channels of bovine chromaffin cells. *J Physiol* 516: 421–432, 1999.
- White EL.** Identified neurons in mouse SmI cortex which are postsynaptic to thalamocortical axon terminals: A combined Golgi-electron microscopic and degeneration study. *J Comp Neurol* 181: 627–662, 1978.